The Astronomical Journal, 124:3393–3399, 2002 December

MEDIUM-RESOLUTION STELLAR SPECTRA IN THE *L* BAND FROM 2400 TO 3000 cm^{-1} (3.3 TO 4.2 MICRONS)

Lloyd Wallace and Kenneth Hinkle
National Optical Astronomy Observatory,[1] P.O. Box 26732, Tucson, AZ 85726;
wallace@noao.edu, hinkle@noao.edu
Received 2002 August 7; accepted 2002 September 17

ABSTRACT

We present a brief atlas of *L*-band (3.3–4.2 μm) spectra for 42 stars plus the Sun and a sunspot observed at a resolving power of $R \sim 3000$. This contribution is intended to supplement our previous *K*-band, *H*-band, and *J*-band spectral atlases. The *L*-band data, which cover some or all of the 2400 to 3000 cm^{-1} (3.3–4.2 μm) region, are mainly for luminous late-type stars. In reducing these data, special care has been taken to remove telluric features, especially water vapor. We identify temperature- and luminosity-sensitive atomic and molecular indices to aid in the classification of stellar spectra in the *L* band. The data are available electronically.

Key words: infrared radiation — stars: fundamental parameters

1. INTRODUCTION

In three previous atlases (Wallace & Hinkle 1996; Meyer et al. 1998; Wallace et al. 2000) we presented medium-resolution near-infrared spectra from the *J*, *H*, and *K* regions for a sample of MK standard stars. Such medium-resolution infrared spectra have many applications. With the completion of recent infrared sky surveys, e.g., 2MASS (Skrutskie et al. 1997) and DENIS (Epchtein 1997), the near-infrared colors for point sources are available over the entire sky to a relatively faint limiting magnitude. For many sources spectroscopic follow-up observations are the next step. Atlases of medium-resolution spectra not only permit spectral classification for normal stars entirely from infrared observations, but also provide a map for planning observations with specific astrophysical goals. We have attempted to make our atlases as useful as possible by providing identifications of spectral lines, as well as spectral indices for classification.

The *J*, *H*, *K* regions have relatively little thermal infrared contribution and hence are relatively easily observed. At wavelengths longer than about 2.5 μm thermal background from the telescope and sky dominates the stellar signal. Until very recently, little work had been done in the 4 μm region compared with the 1–2.5 μm near-infrared. Surprisingly, the first atlas of stellar spectra in the near-infrared included the 4 μm region. Johnson & Mendez (1970) presented spectra of 32 stars of spectral type A0–M7, as well as some carbon stars from 1 to 4 μm at resolving powers varying from 300 to 1000. A review of early work in infrared stellar spectroscopy is given by Merrill & Ridgway (1979). Fourier transform spectrometer (FTS) spectroscopy, which will be discussed in this paper, was the next step forward in infrared spectroscopy, allowing much improved sensitivity with broad wavelength coverage. Ridgway et al. (1984) present an atlas of FTS spectra of five stars observed at high resolution from 3.60 to 4.17 μm.

A major advance in mid-infrared astronomy resulted from space based observations. The *IRAS* and *Infrared Space Observatory* (*ISO*) missions both resulted in a considerable body of mid-infrared spectra at medium to low resolution. The 3 and 4 μm region is near the border of the thermal infrared, and since it is observable from the ground it lacks the scientific justification of longer wavelengths. However, *ISO* did include a short-wavelength spectrometer that covered 2.4–45.2 μm (Kessler et al. 1996; de Graauw et al. 1996), and these data are now publicly available.

Here we present an atlas of stellar spectra from 2400 to 3000 cm^{-1} (3.3 to 4.2 μm) to complement and extend our previous near-infrared work. The sample described here is much less extensive than our other atlases. In fact all the spectra were observed for other purposes. However, we have been able to produce a uniform set of spectra. There are enough data to provide some overlap between ground- and space-based surveys. In § 2 and 3, we describe the observations and the data reduction. In § 4, we present the spectra and detail the identification of spectral features observed. In § 5 we discuss the combined 1.05 to 4.2 μm spectrum for a few stars that we have observed in the *L*, *K*, *H*, and *J* bands. A general discussion can be found in § 6.

2. OBSERVATIONS

The data were collected from archival spectra taken with the FTS at the Kitt Peak National Observatory 4 m telescope. This FTS was designed for observing stellar sources and featured dual inputs and dual outputs for maximum sky cancellation and efficiency (Hall et al. 1979). The observations discussed here span 1977 through 1987. The FTS was closed in 1995 as a result of observatory budget reductions. While the observing process has been described in previous articles of this series (see especially Meyer et al. 1998), these papers were concerned with the *J*-*H*-*K* near-infrared. Procedures for observing in the thermal infrared are summarized in this section.

Interferograms were sampled at 1 kHz in alternately forward and backward scan directions as the path difference was continuously varied up to the maximum path difference set by the spectral resolution. One interferogram typically required two to three minutes to observe. A complete observation, which consisted of tens of pairs of co-added interferograms, required hours. A few of the observations reported here used dichroics in the output arms of the FTS

[1] Operated by the Association of Universities for Research in Astronomy, Inc., under cooperative agreement with the National Science Foundation.

to separate portions of the interferogram longward and shortward of 2.5 μm. The interferogram was then recorded using separate detectors equipped with the appropriate *L*- and *K*- or *H*-band filters.

The program star was centered in a 2.″7 aperture, and sky was observed simultaneously in an identical aperture offset by 50″. Data were obtained in a beam-switching mode (A-B-B-A), alternating the source position between the two input apertures. The interferograms were co-added, keeping the opposite scan directions separate but combining information with the source in different apertures. The dual-input FTS design results in the spectrum of the background emission (obtained from the offset aperture) being subtracted from the interferogram of the star plus sky spectrum in Fourier space as the data are collected. This, combined with the beam switching, very effectively canceled the background radiation, allowing moderately broadband observations in the thermal infrared.

Unlike the other articles in this series, the spectra described here come from a mixed lot, having been originally observed with different bandpass filters and at different resolutions. Two different blocking filters were used to observe the 4 μm region. One filter, the one used by Ridgway et al. (1984), is a more narrow filter covering 2400 to 2800 cm^{-1}. The second filter is broader, giving a range 2400 to 3000 cm^{-1}. For background noise–limited observations with an FTS, the noise results from the background signal over the entire filter bandpass. Thus in the 4 μm region the more narrow filter gave better signal-to-noise ratio in an equal integration time and, hence, was more extensively used.

3. REDUCTIONS

The interferogram data, which are recorded as intensity as a function of position, were Fourier transformed to produce spectra. As a result the natural units of these spectra are relative flux as a function of wavenumber (σ cm^{-1}). Following transforming of the data the two spectra resulting from backward and forward scan directions were combined. Comparison of the spectra from backward and forward scanned data serves as a first defense against bad data.

Since the spectra were obtained with a range of instrument configurations, the next step in the reductions was processing to a common apodized resolution of 0.90 cm^{-1} and a common sampling of 0.220 cm^{-1} per sample, with the first sample at 2200.00 cm^{-1}. Fourier transform spectra can be reduced in resolution by convolution with an apodizing function (Norton & Beer 1976). For best comparison with spectra obtained using other instruments, we selected a Gaussian apodizing function. The point spacing and sampling for the data were determined by sample parameters entered by the observer. To set a common point spacing it was necessary to interpolate. A linear interpolation routine was employed.

As the primary reference for the removal of the telluric spectrum, spectra of IRC+10216 have been used. These spectra were usually, but not always, obtained on the same night as the program star. Ratios of spectra of IRC+10216 obtained on different nights with the same instrumental configuration frequently show low-frequency, low-amplitude ripple, presumably due to subtle changes in the instrument optical alignment. To avoid the resulting errors we have selected, wherever possible, spectra of IRC+10216 obtained on the same night as the program star even though the air-mass match was not necessarily optimal. As partial compensation for the large variation of the intensity of IRC+10216 with wavelength, the IRC+10216 spectra have been divided by a blackbody distribution at 400 K. The 400 K blackbody temperature was set empirically to produce spectra that were quasi-normalized over the 2400 to 3000 cm^{-1} region.

It is well known that water has a different scale height and temporal variability in the earth's atmosphere from the other telluric gasses. A further corrective step was taken to remove any residual telluric signal, in particular water, from the spectra after the ratios were taken. This was done using a logarithmic compression of the ratio of two spectra of IRC+10216 obtained on 1984 Mar 11 and 13 at air masses of 1.21 and 1.91. This simulates a telluric spectrum. Scaling to the residual telluric spectrum and then dividing by this ratio was found to give good correction to the telluric absorption-line spectrum. However, a complication of the 4 μm region is the N_2 pressure-induced band centered near 4.2 μm (Wing & Rinsland 1979). The pressure-induced dipole absorption scales with the square of pressure rather than with pressure, as is the case for the other telluric absorbers. Hence it is not fully removed by the process we have described. We believe this pressure-induced N_2 absorption accounts for the trend of the continua of some reduced spectra to higher or lower levels at the long-wavelength limit of our spectra.

Careful examination of our reference IRC+10216 spectra supported the conclusion of Ridgway et al. (1984) that the IRC+10216 spectrum has no detectable intrinsic 3.3 to 4.2 μm absorption features. However, Cernicharo et al. (1999) have detected a number of 1% to 2% deep features in a 3 and 4 μm *ISO* spectrum of IRC+10216. We believe that these features are in the noise in the data discussed here. We find no indication of a residual IRC+10216 spectrum as pseudo-emission in any of the reduced spectra. The IRC+10216 lines cannot be seen on $R = 100{,}000$ FTS spectra and most likely are intrinsically weak lines and not intrinsically narrow, deep circumstellar lines observed at low resolution. The 1.6 to 2.5 μm spectrum of IRC+10216 has a rich spectrum of weak features that is believed to be the scattered photospheric spectrum (Hinkle & Keady 2000).

Some of the spectra reduced as described above had poor signal-to-noise ratio, some had severe continuum distortion, and for some of the broad filter spectra it was not possible to achieve good telluric correction. Setting aside these spectra, as well as duplicates that add no additional information, Table 1 gives a list of 45 good reductions. These reduced spectra are available electronically from the NOAO web site data archive. Two solar spectra are also presented, one of the disk center from Livingston & Wallace (1991), and a second of a sunspot from Wallace & Livingston (1992). Both spectra have been apodized to low resolution as described above. At medium resolution, previous comparisons of solar disk center spectra with solar integrated disk spectra have shown the spectra to be indistinguishable.

We have selected spectra from the reduced sample to make up a "grid" across the H-R diagram. These spectra are shown in Figures 1, 2, and 3. Figures 4 and 5 illustrate a sample of peculiar late-type star spectra. As noted earlier the data were drawn from archival spectra, mainly observed at high resolution. Hence the sample is heavily weighted to

TABLE 1
LIST OF REDUCED SPECTRA

Star	Name	Spectrum	Reference	Dates
HR 90	R And[a]	S5/4.5e	1	1977 Oct 21
HR 681	o Cet[a]	M7 III	2	1977 Oct 21
HR 867	RZ Ari	M6– III	3	1987 Oct 2
HR 1457	α Tau	K5+ III	3	1977 Oct 21
HR 1612	ζ Aur	K4 II + B8 V	2	1984 Mar 12
HR 1648	W Ori	C–N5	4	1987 Jan 23
HR 1845	119 Tau	M2 Iab–Ib	3	1987 Oct 2
HR 2061	α Ori	M1–M2 Ia–Iab	3	1977 Oct 21, 1987 Oct 2
HR 2286	μ Gem	M3 IIIab	3	1977 Oct 21
HR 2473	ϵ Gem	G8 Ib	3	1984 Mar 13
HR 2508	...	M1+ Ib–IIa	3	1984 Mar 10
HR 3639	RS Cnc	M6 IIIa	2	1984 Mar 10, 1987 Oct 2
HR 3748	α Hya	K3 II–III	3	1982 Feb 9
HR 4483	ω Vir	M4 III	2	1984 Mar 11
HR 4608	o Vir	G8 IIIa	3	1984 Mar 11
HR 4846	Y CVn	C–J4.5	4	1987 Apr 15
HR 4910	δ Vir	M3+ III	3	1987 Apr 16
HR 5226	10 Dra	M3.5 III	3	1984 Mar 10
HR 5299	BY Boo	M4.5 III	3	1984 Mar 12
HR 5340	α Boo	K1.5 III	3	1982 Feb 9
HR 5563	β UMi	K4– III	3	1982 Feb 9
HR 5589	RR UMi	M4.5 III	3	1984 Mar 10
HR 5854	α Ser	K2 IIIb	3	1984 Mar 13
HR 6134	α Sco	M1.5 Iab–Ib	3	1983 Aug 22
HR 6146	30 Her	M6– III	3	1987 Apr 15
HR 6406	α^1 Her	M5 Ib–II	3	1983 Aug 23
HR 6702	OP Her	M5 IIb	2	1987 Apr 15
HR 6705	γ Dra	K5 III	3	1982 Feb 9
HR 7001	α Lyr	A0 Va	5	1983 Aug 22
HR 7139	δ^2 Lyr	M4 II	3	1984 Mar 10
HR 7405	α Vul	M0.5 IIIb	3	1987 Apr 15
HR 7442	V1743 Cyg	M4.5 III	2	1984 Mar 10
HR 7564	χ Cyg[a]	S6+/1e	1	1977 Oct 21
HR 8775	β Peg	M2.5 II–III	3	1983 Aug 22
HR 9004	TX Psc	C–N5	4	1987 Jan 22
HD 1546	VX And	C–J4.5	4	1987 Jan 23
HD 22611	U Cam	C–N5	4	1987 Jan 23
HD 112559	RY Dra	C–J4$^-$	4	1987 Apr 15
HD 114961	SW Vir	M7 III	3	1987 Jul 9
HD 126327	RX Boo	M7.5–M8 III	3	1987 Jul 9
HD 183556	UX Dra	C–N5	4	1984 Mar 10, 1987 Apr 15
...	V Cyg[a]	Ce, pec	6	1977 Oct 21

[a] AAVSO phases for Miras: R And, 0.67; o Cet, 0.87; χ Cyg, 0.17; V Cyg, 0.60.

REFERENCES.—Spectral types were obtained from the following sources: (1) Keenan & Boeshaar 1980; (2) Hoffleit & Jaschek 1982; (3) Keenan & McNeil 1989; (4) Barnbaum, Stone, & Keenan 1996; (5) Morgan, Abt, & Tapscott 1978; (6) our estimate.

bright stars. In the 4 μm region "bright" is frequently synonymous with "cool," as well as with "luminous," and the sample consists largely of spectral type K or later. Less luminous stars, especially dwarfs, are not well represented.

4. SPECTRAL IDENTIFICATIONS

The identifications of the spectral features rest heavily on the analysis by Ridgway et al. (1984) of high-resolution spectra. The sample of Ridgway et al. (1984) includes spectra of oxygen- and carbon-rich stars and so is similar to our set of spectra.

For the oxygen-rich giants and supergiants (Figs. 1 and 2), the heads of the 2-0, 3-1, 4-2, and 5-3 vibration-rotation bands of SiO and the *P*-branch lines of the 1-0 and 2-1 vibration-rotation bands of OH are very clear. Each *P*-branch feature labeled consists of four lines, due to Λ-doubling and spin splitting, which are of similar intensity, with the center two unresolved and the outer two separated by 3 or 4 cm^{-1}. For otherwise unblended features this gives the appearance of a trident, as in the case of the P19 feature of the 1-0 band. Weaker *P*-branch features of the 3-2 and 4-3 bands are also present. The only prominent atomic feature is the Mg I blend at 2585 cm^{-1}. A weaker Mg I line contributes to the blend at 2433 cm^{-1}. A Ca I blend at 2704 cm^{-1} contributes as much to the 2704 cm^{-1} feature as does the OH 3-2 P13 blend.

The dwarf star spectra (Fig. 3) cover a more extended temperature range than the giant and supergiant spectra. Vega shows only H lines, with Brackett α ($n = 4$–5) and

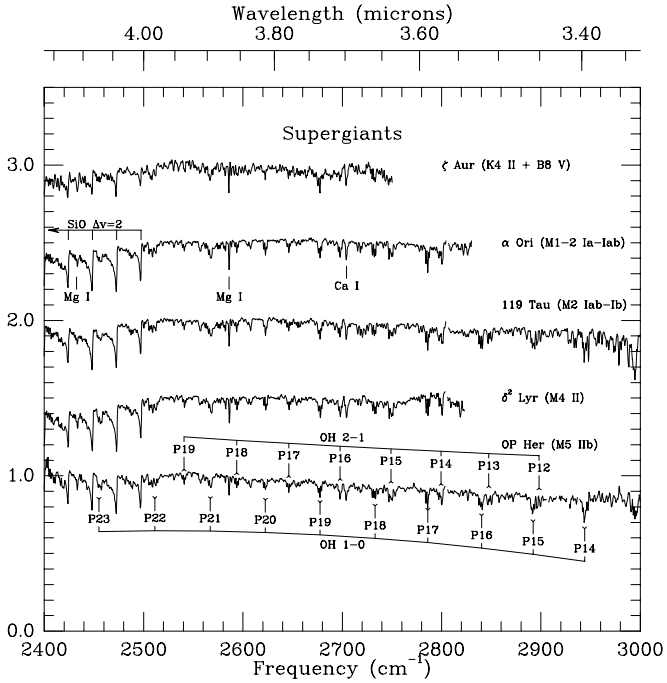

FIG. 1.—Representative spectra of supergiants. The labeled SiO features are band heads, whereas the OH features are blends of four *P*-branch lines with quantum number *N* indicated. The labeled features appear in all five of the spectra, but with different strengths. Each spectrum has been shifted vertically by 0.5.

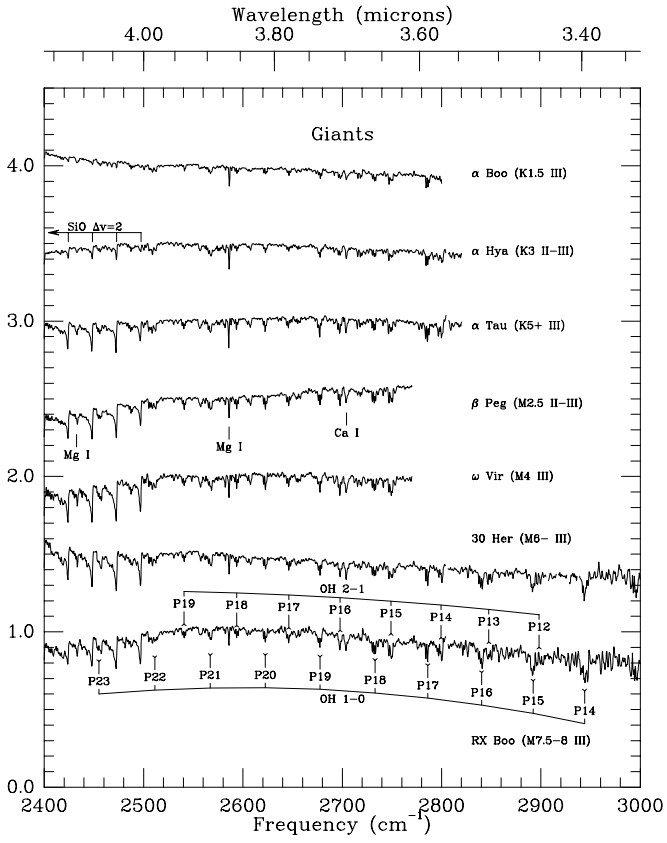

FIG. 2.—Same as Fig. 1, but for giants

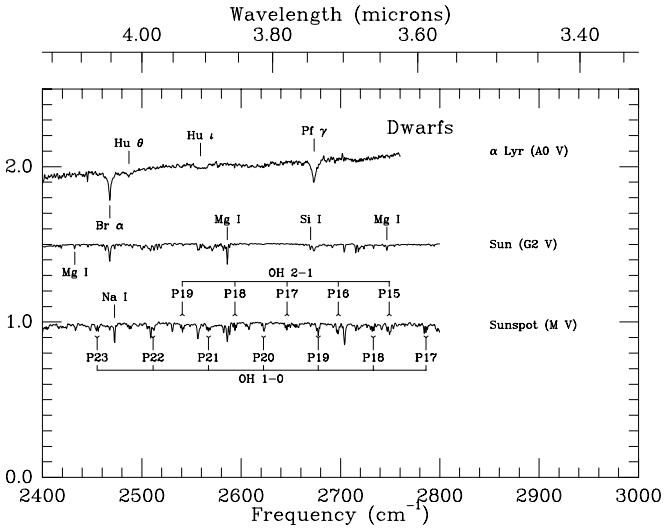

FIG. 3.—Representative spectra of dwarf stars. The hydrogen series lines Brackett α, Pfund γ, and Humphreys θ are clearly present in the α Lyr spectrum. Humphreys ι is possibly also present. The molecular and atomic labels are as in Figs. 1 and 2. The solar spectrum is disk center. The sunspot spectrum serves as a proxy for an early M dwarf.

Pfund γ ($n = 5$–8) clearly present. Humphreys θ ($n = 6$–14; Garcia & Mack 1965) is also present. Humphreys η ($n = 6$–13) at 2398 cm^{-1} is at the edge of the data. Humphreys ι ($n = 6$–15) could be involved in the broad feature at 2560 cm^{-1}. The other dwarf spectra are taken from solar data. The solar center-of-disk spectrum combines the hydrogen spectrum with the atomic blends seen in the giants. The sunspot spectrum, equivalent at this resolution to an early M dwarf spectrum since the Zeeman splitting is unresolved, no longer has hydrogen lines present. OH has become strong. A conspicuous difference between the sunspot and M giant or supergiant spectra is that the SiO bands are absent in the former.

Of the carbon stars (Fig. 4), W Ori and TX Psc show the heads of the 2-0, 3-1, 4-2, and 5-3 vibration-rotation bands of CS. These two spectra and the spectrum of the carbon star VX And also show *P*- and *R*-branch features of the CH 1-0 vibration-rotation band and the *R*-branch features of the 2-1 band. The ground states of both CH and OH are $^2\Pi$, but the CH features are sharper than the OH and do not have the trident shape. Based on their high-resolution spectra, Ridgway et al. (1984) state that away from the CS bands most of the line opacity is due to CN. V Cyg appears to be featureless. The IR colors of V Cyg indicate that it is obscured by dust.

In the Mira spectra at medium resolution (Fig. 5), only SiO is prominent. The Mg I and Ca I lines also appear in χ Cyg, and the OH features that are prominent in the supergiants are also weakly apparent. A complication for χ Cyg and R And is the HCl vibration-rotation lines, which present both emission and absorption features. Although not individually apparent at medium resolution because emission and absorption equivalent widths are similar, overlap of the profiles confuses the appearance of the OH. The presence of emission and absorption confuses the appearance of the SiO spectrum at some Mira phases (Lebzelter, Hinkle, & Aringer 2001). Aringer et al. (1999), Rinsland & Wing (1982), and Hinkle et al. (1976) all report that SiO is strongly phase dependent.

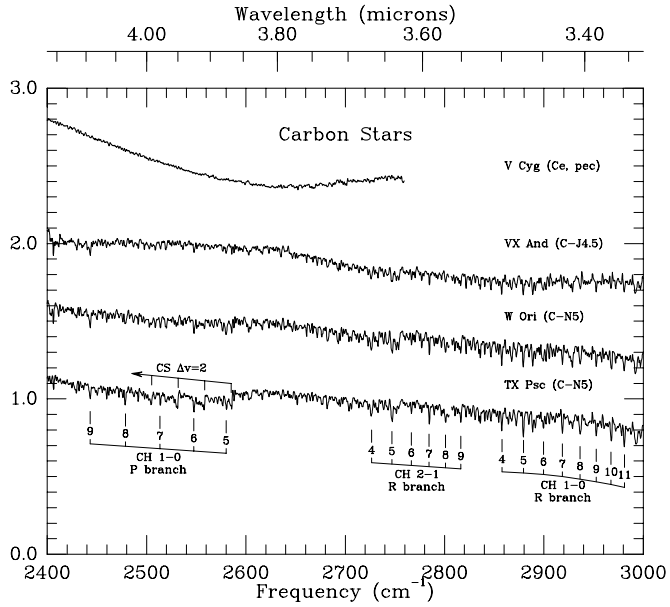

FIG. 4.—Spectra of carbon stars. V Cyg appears featureless. The other three clearly show *P*- and *R*-branch lines of CH, and TX Psc shows CS band heads.

A further complexity in 4 μm spectra of very cool stars is the presence of H_2O. Examination of the spectrum of o Cet observed at high resolution shows that it is dominated by a complex rich spectrum, which we assume is H_2O. Lebzelter et al. (2001) report on the identification of individual lines. The presence of a complex absorber is also apparent at medium resolution.

We have measured the strengths of four indices for use in spectral classification. These are defined in Table 2. In each case the continuum has been defined by linear interpolation between points on each side of the feature. After normalization to this level the residual intensity was integrated over the feature. The SiO index includes most of the 2-0 band and the Mg I index contains only the Mg I feature. The OH 1-0 P22 index also contains the OH 3-2 P17 blend plus weaker atomic features. The OH 1-0 P19 index could be influenced by a Mg-K blend at 2676.9 cm^{-1}. Values for each index in each star appear in Table 3.

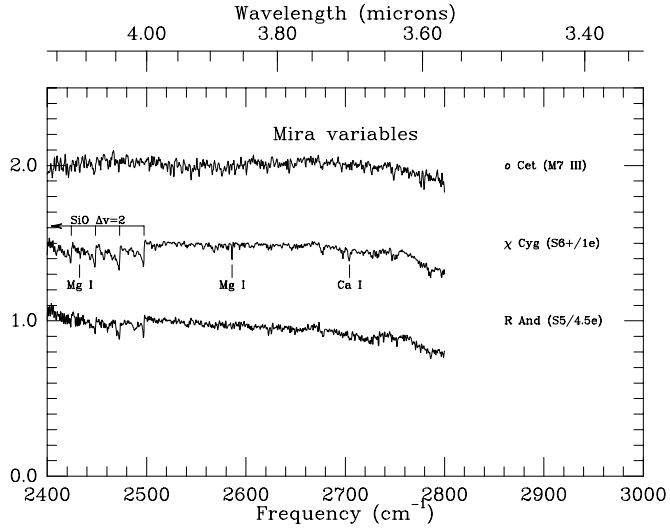

FIG. 5.—Spectra of Mira variables. SiO is prominent in two of these spectra, but other authors have shown that these bands are highly phase-dependent in Miras (see text).

TABLE 2
CONTINUUM POINTS AND BAND LIMITS FOR *L*-BAND SPECTRAL INDICES

Feature	Continuum Points[a]	Band Limits[a]
SiO 2-0 band	2473.8, 2498.7	2475.9 to 2497.7
Mg I 2586 cm^{-1}	2583.6, 2587.3	2585.0 to 2587.0
OH 1-0 P22	2503.7, 2517.4	2505.8 to 2515.3
OH 1-0 P19	2666.7, 2682.6	2672.1 to 2680.5

[a] Units are inverse centimeters.

The spectral indices derived from the 4 μm region appear to be useful for spectral classification. Adopting the Meyer et al. (1998) spectral type to effective temperature conversion as a function of luminosity class, Figure 6 shows equivalent-width indexes as a function of $T_{\rm eff}$. SiO is strongly temperature sensitive. SiO also does not appear in the sunspot spectrum and so must be luminosity sensitive. However, OH appears in sunspots, as well as supergiants, so does not have a strong luminosity sensitivity. The Mg I index appears to be luminosity sensitive. Mg I was a key index in the *J* band (Wallace et al. 2000). Additional obser-

TABLE 3
L-BAND SPECTRAL INDICES

Star	Spectral Type	SiO (cm^{-1})	Mg I (cm^{-1})	P19 (cm^{-1})	P22 (cm^{-1})
ϵ Gem.....	G8 Ib	0.407	0.181	0.361	0.587
α Boo.....	K1.5 III	0.182	0.129	0.262	0.237
α Ser	K2 IIIb	0.668	0.159	0.165	0.325
α Hya.....	K3 II–III	0.281	0.171	0.364	0.333
β UMi.....	K4– III	0.360	0.147	0.345	0.315
ζ Aur.....	K4 II + B8 V	0.578	0.194	0.422	0.624
γ Dra	K5 III	0.499	0.167	0.443	0.315
α Tau	K5+ III	0.783	0.191	0.432	0.399
α Vul.....	M0.5 IIIb	0.764	0.126	0.585	0.430
HR 2508	M+ Ib–IIa	0.892	0.173	0.511	0.517
α Ori 1.....	M1–M2 Ia–Iab	1.421	0.191	0.507	0.427
α Ori 2.....	M1–M2 Ia–Iab	1.126	0.192	0.445	0.511
α Sco.....	M1.5 Iab–Ib	0.941	0.177	0.696	0.476
119 Tau.....	M2 Iab–Ib	1.132	0.188	0.452	0.458
β Peg.....	M2.5 II–III	0.864	0.141	0.427	0.369
μ Gem	M3 IIIab	1.075	0.166	0.465	0.450
δ Vir	M3+ III	1.050	0.171	0.427	0.373
10 Dra.....	M3.5 III	1.118	0.145	0.522	0.351
δ^2 Lyr	M4 II	1.383	0.164	0.569	0.438
ω Vir	M4 III	1.300	0.163	0.564	0.442
BY Boo.....	M4.5 III	1.067	0.174	0.479	0.495
V1743 Cyg	M4.5 III	1.551	0.159	0.544	0.423
RR UMi	M4.5 III	1.080	0.161	0.443	0.345
OP Her.....	M5 IIb	1.186	0.128	0.502	0.426
α^1 Her	M5 Ib–II	1.336	0.159	0.448	0.422
30 Her	M6– III	1.338	0.140	0.407	0.382
RZ Ari	M6– III	1.189	0.177	0.457	0.662
RS Cnc 1	M6 IIIa	1.014	0.131	0.333	0.385
RS Cnc 2	M6 IIIa	1.007	0.132	0.379	0.352
SW Vir	M7 III	1.102	0.135	0.423	0.486
o Cet	M7 III	0.405	0.074	0.122	0.261
RX Boo.....	M7.5–M8 III	1.302	0.123	0.463	0.501

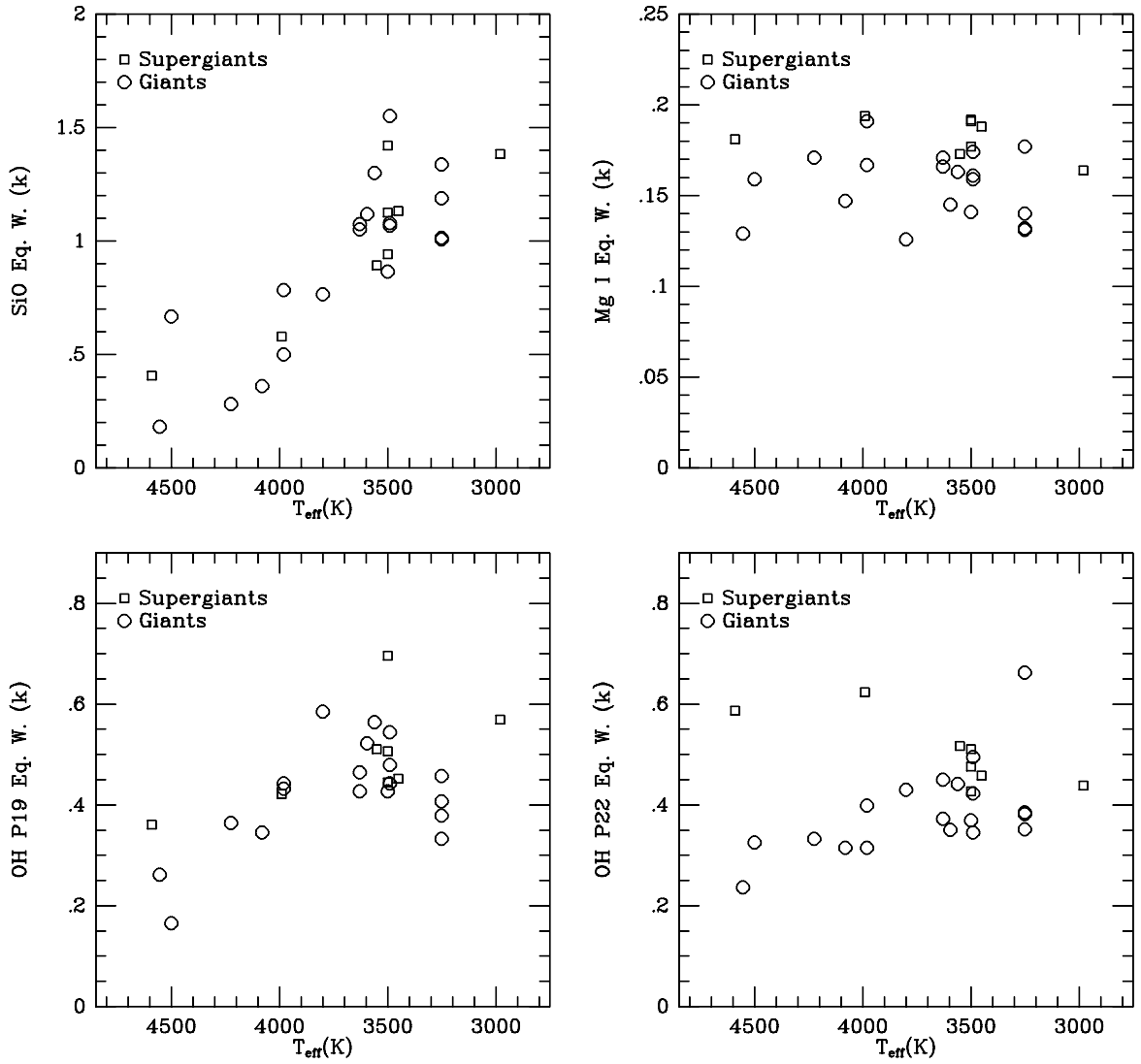

FIG. 6.—Spectral indices plotted as a function of effective temperature. The unit of equivalent width is the kayser (k) = 1 cm^{-1}.

vations over a larger range of the H-R diagram are needed and presumably will soon be available from the *ISO* database (Lenorzer et al. 2002).

5. COMBINED VIEW OF THE 1.05 TO 4.2 MICRON SPECTRAL REGION

For a few of the program stars, medium-resolution spectra of the same stars are presented for other bands in previous articles of this series (Wallace & Hinkle 1996; Meyer et al. 1998; Wallace et al. 2000). We discuss here three stars observed in the *J*, *H*, *K*, and *L* bands. The nominal coverage of these bands was 1.10–1.34, 1.50–1.80, 2.00–2.42, and 3.5–4.2 μm, respectively. Since there are very few stars that were observed in all four bands, the desire to obtain as much range in spectral type as possible led to the selection α Lyr (A0 Va; $T_{\rm eff} = 9480$ K), α Boo (K1.5 III; $T_{\rm eff} = 4550$ K), and α Her (M5 Ib–II; $T_{\rm eff} = 2800$ K). All the spectra have been reduced to a resolving power of 1000 for this comparison. The flux information for these spectra is not available. Rather than presenting the spectra with the continuum normalized, the continuum levels have been adjusted to that of blackbodies at the effective temperatures of the stars. The resulting spectra are illustrated in Figure 7.

For α Lyr, the *L*-band spectrum presented earlier in this paper was used. Since α Lyr was observed as a telluric reference spectrum, it posed special problems in being reduced as a program star. For the *J*, *H*, and *K* bands, ratios of α Lyr spectra at differing air masses were used to correct for telluric absorption. The instrumental response for the bandpass was then removed by dividing the corrected spectrum by a heavily filtered version of the same spectrum. This also removes the stellar energy distribution. The approximate continuum variation was restored by multiplying by a blackbody at 9480 K.

For α Boo we selected the high-resolution atlas spectra of Hinkle, Wallace, & Livingston (1995). The atlas spectra have been corrected for telluric absorption, and the continuum has been normalized. To restore the approximate stellar flux distribution, the spectra were multiplied by a blackbody at 4550 K. Hinkle et al. (1995) made a special effort to maximize spectral coverage by using a number of filters other than the 4 μm filters described here. The resulting spectral coverage is greater than for the other two stars.

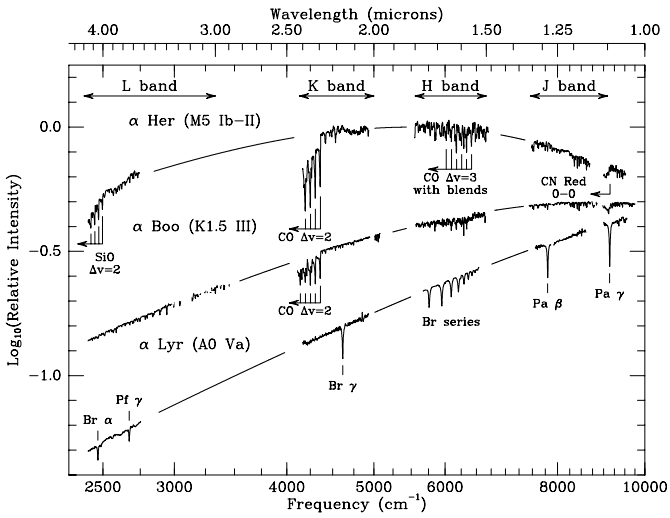

FIG. 7.—Spectra of α Lyr (*bottom*), α Boo (*middle*), and α Her (*top*) in the *J*, *H*, *K*, and *L* bands with the prominent features identified. The relative signal levels and slopes of the *J*, *H*, *K*, and *L* segments result from scaling to a blackbody at the stellar effective temperature (see text). The fluxes and blackbody temperatures used are illustrative. For instance because of subsolar metal abundances, the giant α Boo has a slightly cooler (redder) effective temperature than shown.

However, gaps in the spectrum due to telluric lines in regions of heavy telluric interference, e.g., from 3000 to 3500 cm^{-1}, prevented the reduction of this region to medium resolution.

A variety of sources were used for the α Her data. For the *L* band the reduction presented in this paper was employed. For the *J* and *K* bands the atlas spectra of Wallace et al. (2000) and Wallace & Hinkle (1996), respectively, were used after correcting for the energy distribution of the reference star, α Lyr. An archival FTS spectrum was used for the *H* band. The telluric correction was done using ratios of α Lyr spectra as described above. Note that the *H*-band spectra of α Boo and α Her are dominated by numerous intrinsic features and not noise (Meyer et al. 1998).

6. DISCUSSION

Comparison of the current data with previous and current results in the literature allows some evaluation of the quality. Comparison with Johnson & Mendez (1970) shows that while the Johnson & Mendez (1970) spectra have remarkable wavelength coverage for their time, the signal-to-noise ratio and resolution of these spectra in the 4 μm region are so poor that frequently the spectra contain little information. On the other hand the spectra presented here have very restricted wavelength coverage compared with those observed with *ISO* (see for instance Figs. 5 and 6 of Lenorzer et al. 2002). The *ISO* spectra, which did not have to be processed to remove the telluric spectrum, also can show very weak spectral features, as is the case in the *ISO* spectrum of IRC+10216 (Cernicharo et al. 1999).

A number of papers have discussed *ISO* spectra of carbon stars. One star observed by *ISO*, TX Psc, is in the current atlas. The *ISO* observation of TX Psc at resolution 2000 (Aoki, Tsuji, & Ohnaka 1998) is quite similar to the spectrum shown in this paper with, of course, the exception that the *ISO* wavelength coverage is much larger. While carbon stars have highly blended spectra, the CH and CS features are conspicuous in both spectra. On the other hand at $R = 400$, the *ISO* spectra of the 3.3 to 4.2 μm region become nearly featureless, showing just a broad shallow dip (Jørgensen, Hron, & Loidl 2000). We also note that the appearance of carbon star spectra in the infrared is quite sensitive to the CNO group abundances. TX Psc does not show HCN and C_2H_2 features in the 3.3 to 4.2 μm region. These features are weakly present in IRC+10216 but are very obvious in spectra of R Scl (Hron et al. 1998).

L. W. is grateful to the NOAO emeritus program for providing office space and computer access. We are indebted to Robert Wing for a careful review of the manuscript. This research made use of the SIMBAD database operated by CDS in Strasbourg, France and NASA's Astrophysics Data System Bibliographic Services.

REFERENCES

Aoki, W., Tsuji, T., & Ohnaka, K. 1998, A&A, 340, 222
Aringer, B., Höfner, S., Wiedemann, G., Hron, J., Jørgensen, U. G., Käufl, H. U., & Windsteig, W. 1999, A&A, 342, 799
Barnbaum, C., Stone, R. P. S., & Keenan, P. C. 1996, ApJS, 105, 419
Cernicharo, J., Yamamura, I., González-Alfonso, E., de Jong, T., Heras, A., Escribano, R., & Ortigoso, J. 1999, ApJ, 526, L41
de Graauw, T., et al. 1996, A&A, 315, L49
Epchtein, N. 1997, in The Impact of Large-Scale Near-IR Sky Surveys, ed. F. Garzon, N. Epchtein, A. Omont, B. Burton, & P. Persi (Dordrecht: Kluwer), 15
Garcia, J. D., & Mack, J. E. 1965, J. Opt. Soc. Am., 55, 654
Hall, D. N. B., Ridgway, S. T., Bell, E. A., & Yarborough, J. M. 1979, Proc. SPIE, 172, 121
Hinkle, K. H., Barnes, T. G., Lambert, D. L., & Beer, R. 1976, ApJ, 210, L141
Hinkle, K. H., & Keady, J. 2000, in The Carbon Star Phenomenon, ed. R. F. Wing (Kluwer: Dordrecht), 537
Hinkle, K., Wallace, L., & Livingston, W. 1995, Infrared Atlas of the Arcturus Spectrum, 0.9–5.3 μm (San Francisco: ASP)
Hoffleit, D., & Jaschek, C. 1982, Bright Star Catalog (4th ed.; New Haven: Yale Univ. Obs.)
Hron, J., Loidl, R., Höfner, S., Jørgensen, U. G., Aringer, B., & Kerschbaum, F. 1998, A&A, 335, L69
Johnson, H. L., & Mendez, M. E. 1970, AJ, 75, 785
Jørgensen, U. G., Hron, J., & Loidl, R. 2000, A&A, 356, 253
Keenan, P. C., & Boeshaar, P. C. 1980, ApJS, 43, 379
Keenan, P. C., & McNeil, R. C. 1989, ApJS, 71, 245
Kessler, M. F., et al. 1996, A&A, 315, L27
Lebzelter, T., Hinkle, K. H., & Aringer, B. 2001, A&A, 377, 617
Lenorzer, A., Vandenbussche, B., Morris, P., de Koter, A., Geballe, T. R., Waters, L. B. F. M., Hony, S., & Kaper, L. 2002, A&A, 384, 473
Livingston, W., & Wallace, L. 1991, An Atlas of the Solar Spectrum in the Infrared from 1850 to 9000 cm^{-1} (1.10 to 5.4 μm) (NSO Tech. Rep. 91-001) (Tucson: NSO)
Merrill, K. M., & Ridgway, S. T. 1979, ARA&A, 17, 9
Meyer, M. R., Edwards, S., Hinkle, K. H., & Strom, S. E. 1998, ApJ, 508, 397
Morgan, W. W., Abt, H. A., & Tapscott, J. W. 1978, Revised MK Spectral Atlas for Stars Earlier Than the Sun (Williams Bay: Yerkes Obs.)
Norton, R. H., & Beer, R. 1976, J. Opt. Soc. Am., 66, 259
Ridgway, S. T., Carbon, D. F., Hall, D. N. B., & Jewell, J. 1984, ApJS, 54, 177
Rinsland, C. P., & Wing, R. F. 1982, ApJ, 262, 201
Skrutskie, M. F., et al. 1997, in The Impact of Large-Scale Near-IR Sky Surveys, ed. F. Garzon, N. Epchtein, A. Omont, B. Burton, & P. Persi (Dordrecht: Kluwer), 25
Wallace, L., & Hinkle, K. 1996, ApJS, 107, 312
Wallace, L., & Livingston, W. 1992, An Atlas of a Dark Sunspot Umbral Spectrum from 1970 to 8640 cm^{-1} (1.16 to 5.1 μm) (NSO Tech. Rep. 92-001) (Tucson: NSO)
Wallace, L., Meyer, M., Hinkle, K. H., & Edwards, S. 2000, ApJ, 535, 325
Wing, R. F., & Rinsland, C.P. 1979, AJ, 84, 1235